

EQUIVALENT FRAME ANALYSIS OF FLAT PLATE BUILDINGS FOR SEISMIC LOADING

By Y. H. Luo,¹ Associate Member, ASCE, A. J. Durrani,² Member, ASCE, and J. P. Conte,³ Associate Member, ASCE

ABSTRACT: An equivalent frame approach is presented for nonlinear seismic analysis of reinforced-concrete flat plate buildings. The approach employs a parametric hysteretic model and is based on the effective slab-width concept. Unlike in the previous equivalent frame approaches, the proposed method targets both the moment-transfer capacity as well as stiffness of the interior and exterior slab-column connections. The hysteretic parameters and the effective slab width factors are determined from results of laboratory tests on slab-column connections for the class of flat plate buildings constructed prior to the 1960s with reinforcing detail typical of gravity load design. The validity of the approach is justified by comparing the calculated and the measured responses of two-bay flat plate subassemblies tested under earthquake-type loading. With the proposed equivalent frame approach, the response of flat plate buildings for seismic loading could be predicted more realistically over a wide range of lateral drift levels.

INTRODUCTION

The eastern region of the United States has a large number of older flat plate buildings which were designed and built to resist gravity loads only. The slab-column connections in these buildings have reinforcing detail appropriate for gravity load design and thus may not have the capacity to sustain deformation reversals during an earthquake of moderate intensity. The study presented here is focused on evaluating the seismic response of flat plate buildings constructed prior to nineteen sixties (ACI: *Building* 1941; ACI: *Building* 1956). The modern seismic codes (UBC: *Uniform* 1991; ACI: *Building* 1989) ensure the safety of flat plate buildings by stipulating three main requirements: (1) Provide adequate moment and shear capacity at connections; (2) limit the demand on connections by requiring lateral load resisting elements such as shearwalls; and (3) have the slab bottom reinforcement continuous through the column as a protection against progressive collapse. Most of the older flat slab and flat plate buildings are deficient in all three counts, especially in the last category. Recent concern over the probability of a moderate intensity earthquake in the eastern United States has spawned interest in studying the seismic resistance and the need for retrofit of these types of buildings.

Being a topic of recent interest, the research data on seismic resistance of slab-column connections and on analytical modeling for seismic response analysis of pre-1960s flat plate buildings is rather limited. Even though several analytical methods, including finite element and equivalent frame approaches, have been used for flat plate systems subjected to static gravity and lateral loads, none of them is appropriate for analyzing older flat plate

¹Grad. Student, Dept. of Civ. Engrg., Rice Univ., P.O. Box 1892, Houston, TX 77251.

²Prof., Dept. of Civ. Engrg., Rice Univ., P.O. Box 1892, Houston, TX.

³Asst. Prof., Dept. of Civ. Engrg., Rice Univ., P.O. Box 1892, Houston, TX.

Note. Discussion open until December 1, 1994. To extend the closing date one month, a written request must be filed with the ASCE Manager of Journals. The manuscript for this paper was submitted for review and possible publication on March 18, 1993. This paper is part of the *Journal of Structural Engineering*, Vol. 120, No. 7, July, 1994. ©ASCE, ISSN 0733-9445/94/0007-2137/\$2.00 + \$.25 per page. Paper No. 5841.

systems under seismic loading. The effective beam-width model (Pecknold 1975; Allen and Darvall 1977) and the equivalent column model (Corley et al. 1961; Corley and Jirsa 1970) were developed to predict the stiffness of flat plates under static loads. The hysteretic response and moment-transfer capacity of the slab-column connections under combined gravity and seismic loading is not considered in these models. Other models, such as the eccentric shear stress model (Di Stasio and Van Buren 1960) and the beam analogy model (Park and Islam 1976), have been developed to predict the shear and flexural strength of connections. The separate treatment of strength and stiffness is not appropriate for predicting the seismic response of flat plate buildings. Seismic analysis requires that the strength, stiffness, nonlinearity of the response, and the hysteretic behavior should all be included in the analytical model. This paper presents an analysis approach for predicting the seismic response of pre-1960s flat plate buildings. This approach considers both strength and stiffness equivalence and also includes the hysteretic characteristics of slab-column connections. Test data on slab-column connections is used to identify the hysteretic model parameters and to verify the analytical results based on the equivalent frame approach.

EXPERIMENTAL RESULTS

Results from two series of tests on flat plate connections, designed and detailed according to ACI Building Code (*Building* 1956), are briefly described before presenting the analytical procedure. In the first series of tests, four half-scale slab-column connection subassemblies each consisting of two exterior connections and one interior connection, were tested under quasi-static cyclic loading to study the seismic behavior of slab-column connections designed to resist gravity loads only. Since the study focussed on the response of the slab in the connection region, the columns were designed to remain elastic during lateral loading. Gravity load was applied to the slab to simulate service loads. Further details of this study can be found elsewhere (Durrani and Du 1992). The second series consisted of tests on individual interior and exterior slab-column connections. These connections were tested to establish the hysteretic model, therefore, no gravity load was applied to the slab. Details of the specimens for both test series are given in Table 1. The test setup and reinforcing detail of the individual connections are shown in Figs. 1 and 2, respectively. The discontinuity of the slab bottom reinforcement at the interior connection is to be noted.

The observed moment-curvature response for the two individual interior and exterior connections is shown in Fig. 3. The moment-transfer capacity of the exterior connection decreased rapidly after reaching the peak moment in both loading directions. In addition, the moment-transfer was observed to occur over a relatively small slab width centered on the column. The torsional capacity of the slab edge adjacent to the column controlled the final moment-transfer capacity of the exterior connection. The moment-transfer capacity of the interior connection was significantly different in the two loading directions and did not change much beyond the peak value as indicated by the envelope of the hysteresis loops. The hysteresis loops for both interior and exterior connections are severely pinched. The slab reinforcement yielded first near the column line and, as the lateral drift increased, more slab reinforcement yielded. The sustained moment-transfer capacity, particularly in the negative moment direction, is attributed to increased participation of the slab with the increasing drift levels. Since the slab bottom reinforcement was not continuous through the column, the

TABLE 1. Specimen Configuration and Material Properties

Specimen (1)	Slab		Gravity load (kPa) (4)	f'_c (MPa) (5)	f_y (MPa) (6)	STEEL AREA FOR SLAB (mm ²)			
	h (cm) (2)	d (cm) (3)				Interior		Exterior	
						Top (7)	Bottom (8) ^a	Top (9)	Bottom (10)
IE	11.5	10.2	2.68 (DL)	20.7	379	---	---	855	641
II	11.5	10.2	2.68 (DL)	20.7	379	0 (639)	---	---	---
DNY_1	11.5	10.2	9.58 (DL + 0.3LL)	35.3	372	0 (284)	0 (284)	855	285
DNY_2	11.5	10.2	12.0 (DL + LL)	25.7	372	0 (284)	0 (284)	855	285
DNY_3	11.5	10.2	9.58 (DL + 0.3LL)	24.6	372	0 (639)	0 (639)	855	641
DNY_4	11.5	10.2	9.58 (DD + 0.3LL)	19.1	372	0 (284)	0 (284)	855	285

^aSlab bottom reinforcement not continuous through the column.

Note: 1 mm = 0.039 in.; 1 mm² = 0.00155 sq in.; 1 kN = 0.225 kip; 1 kPa = 0.145 psi.

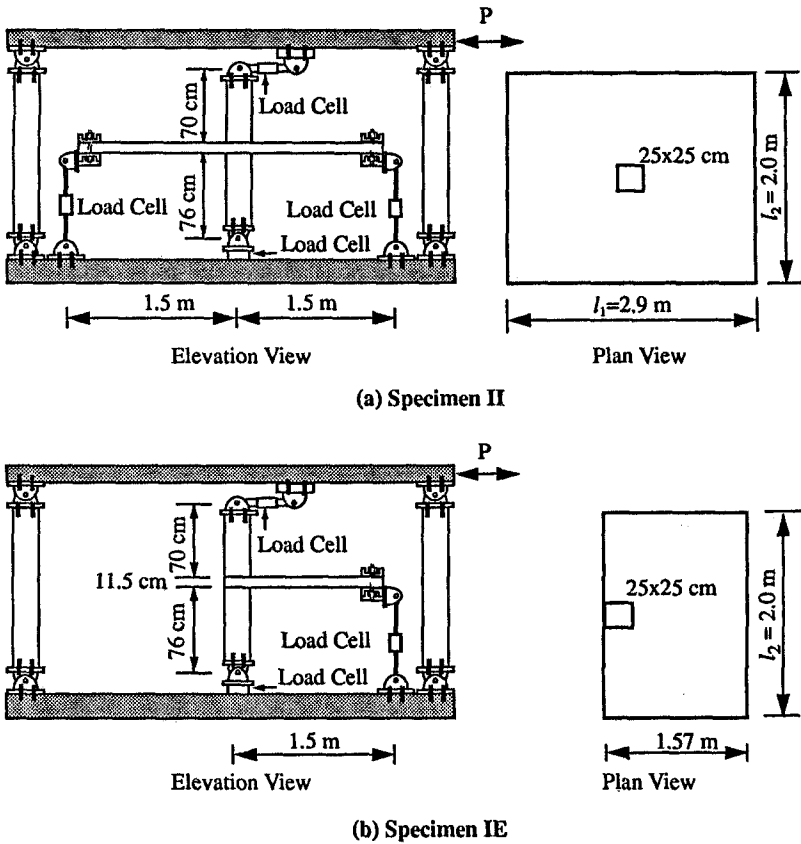
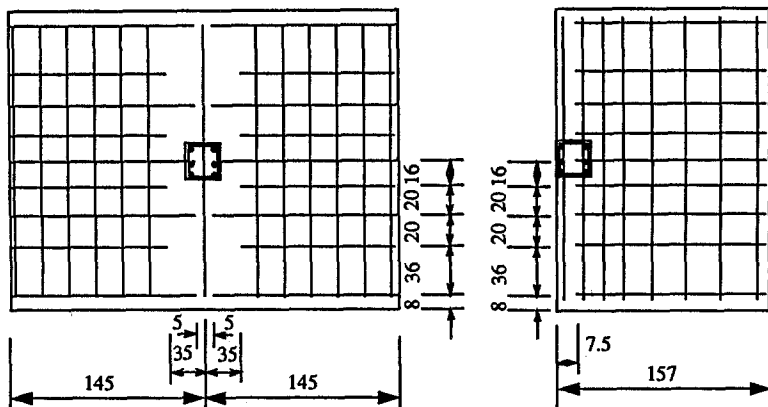


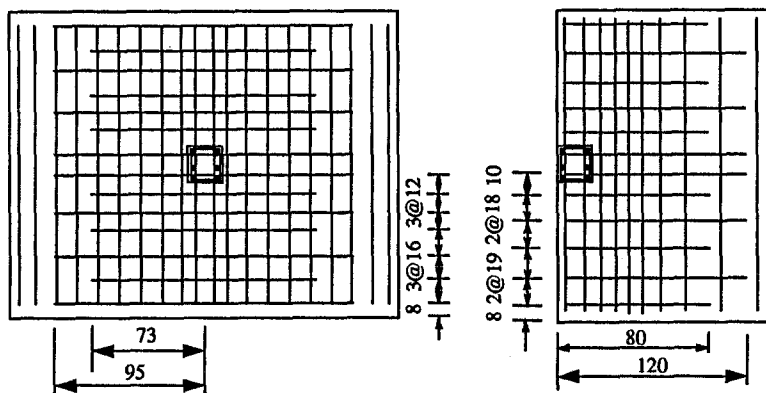
FIG. 1. Test Setup for Individual Connections: (a) Specimen II; (b) Specimen IE

moment-transfer capacity in positive bending was limited to the cracking moment capacity of the slab. The failure of connections is typically characterized by flexural yielding of the slab at the interior connection, and flexural yielding and torsional cracking of the slab edge at the exterior connection. Since no gravity load was applied to the slab in individual connections, the low flexural yielding strength of the slab protected the connection against the possibility of a punching failure.

The slab-column connection subassemblies with two exterior and one interior connection each were subjected to gravity loads as indicated in Table 1. The gravity load on the slab was adjusted to result in the same level of shear stress in the connection region as in the prototype building. The observed moment-curvature response of the interior and exterior connections of the subassembly specimens is shown in Figs. 4 and 5. The moment-curvature behavior of connections in subassemblies is observed to be very similar to that of the individual connections. In positive bending, the moment-transfer capacity of the interior connection was limited to the flexural cracking strength of the slab. The anchorage of the slab bottom reinforcement at the exterior connections was lost quickly under cyclic loading, resulting in rapid degradation of the moment-transfer capacity in positive bending [see Figs. 4(a) and 5(a)]. As in individual connections, the



Bottom reinforcing detail (all slab bars 9.5 mm dia.)



Top reinforcing detail (all slab bars 9.5 mm dia.)

(a) Specimen II

(b) Specimen IE

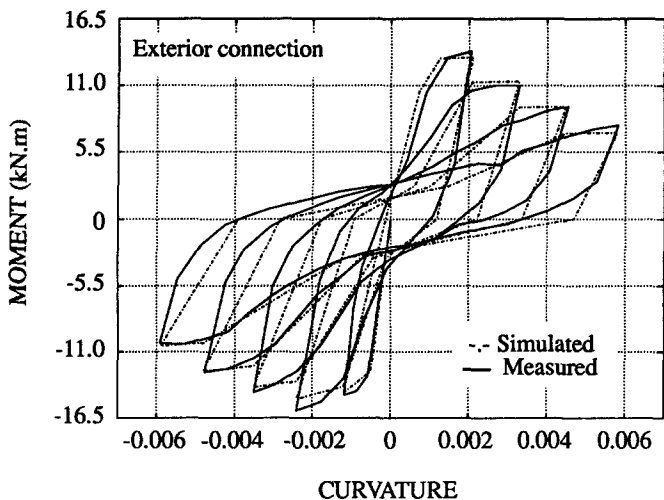
UNIT: cm

FIG. 2. Reinforcing Detail of Individual Connections: (a) Specimen II; (b) Specimen IE

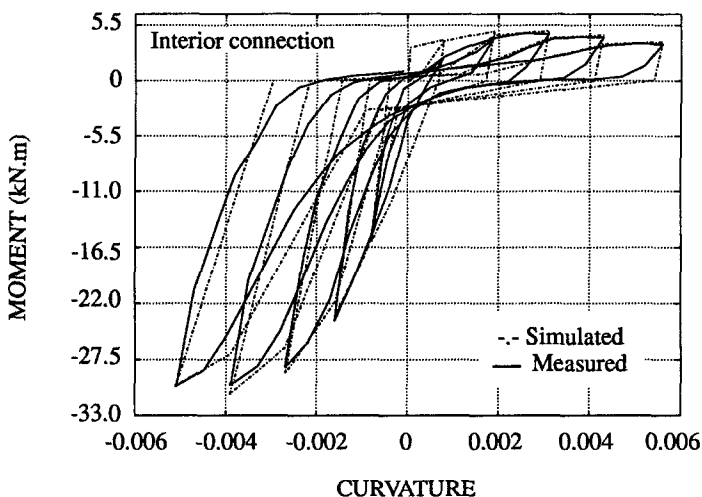
hysteresis loops are severely pinched. The measured moment-transfer capacities of all connections in both positive and negative loading directions are summarized in Table 2.

IDENTIFICATION OF HYSTERETIC PARAMETERS

The parametric model developed by Kunnath et al. (1990) was used in the present study to simulate the hysteretic response of slab-column connections. The rules for inelastic loading reversals in this model are described by three parameters and a nonsymmetric trilinear primary curve. The three hysteretic parameters define stiffness degradation, loss of strength, and pinching of the hysteresis loops. This model has been improved recently by combining the trilinear envelope with four parameters: stiffness degrad-



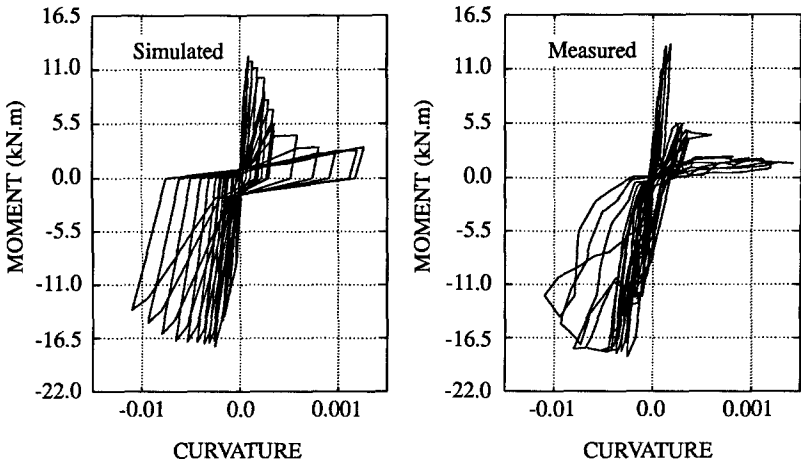
(a) Specimen IE



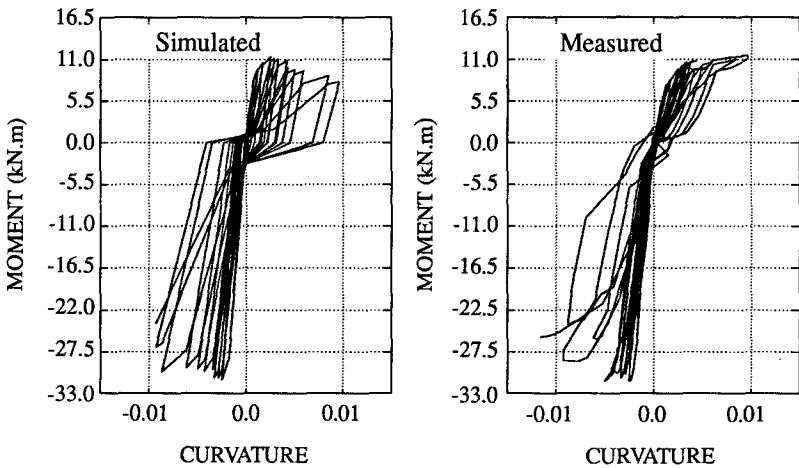
(b) Specimen II

FIG. 3. Simulated and Measured Response of Individual Connections: (a) Specimen IE; (b) Specimen II

ing coefficient (α), energy-based strength deteriorating coefficient (β_1), ductility-based strength deteriorating coefficient (β_2), and target slip or crack-closing parameter (γ), and has been implemented in version 3.0 of IDARC-2D (Kunnath et al. 1992) computer program for nonlinear dynamic analysis of reinforced concrete frame buildings. This program was used in this study to simulate the test results.



(a) Specimen DNY_1's exterior connection



(b) Specimen DNY_1's interior connection

FIG. 4. Simulated and Measured Moment-Curvature Response of DNY_1: (a) Specimen DNY_1's Exterior Connection; (b) Specimen DNY_1's Interior Connection

The hysteretic parameters were identified from the observed moment-curvature loops of the test specimens. These parameters were then verified by comparing the simulated load-drift response with the measured response of the test specimens. Since the simulated load-drift response of the specimens was quite sensitive to the hysteretic parameters, the measured moment-curvature response of the slab-column connections was used to estimate the hysteretic parameters. By simulating the measured moment-curvature loops of all test specimens, the average values of hysteretic parameters were identified as $\alpha = 2.0$, $\beta_1 = 0.02$, $\beta_2 = 0.0$, $\gamma = 0.12$ for slab at interior connections, and $\alpha = 2.0$, $\beta_1 = 0.02$, $\beta_2 = 0.02$, $\gamma = 0.12$ for slab at exterior connections. All parameters for both interior and exterior connec-

tions were the same except for the ductility-based strength deterioration coefficient β_2 . A zero value of this parameter for the interior connections reflects the flat top of the moment-curvature envelope and a value of 0.02 for the exterior connections represents the negative slope of the moment-curvature envelope. A comparison of the simulated moment-curvature loops based on the identified parameters and the measured hysteresis loops is shown in Figs. 3–5. Good agreement between the simulated and the observed hysteresis loops shows reliability of the identified parameters.

EQUIVALENT FRAME APPROACH

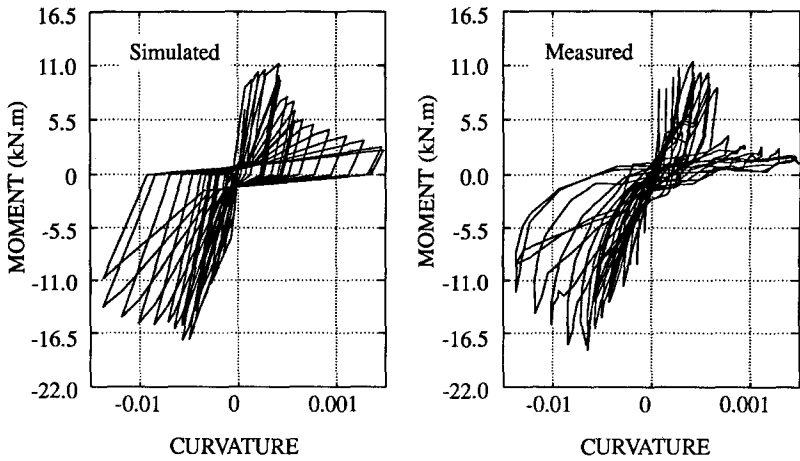
Flat plate structures subjected to combined gravity and lateral loads are typically analyzed by linear elastic finite element and equivalent frame approaches. The three dimensional finite element approach is computationally intensive even for flat plate buildings of moderate heights. Since the flat plate buildings behave inelastically even in earthquakes of moderate intensity, a three-dimensional nonlinear analysis for seismic loading is not practical at present. For these reasons the equivalent frame approach, which is based on an effective slab width or an equivalent column concept, is more widely used and is chosen as the basis for seismic analysis of flat plate buildings in this study. The equivalent frame concepts for two dimensional analysis are briefly reviewed in the following.

Effective Slab-Width Method

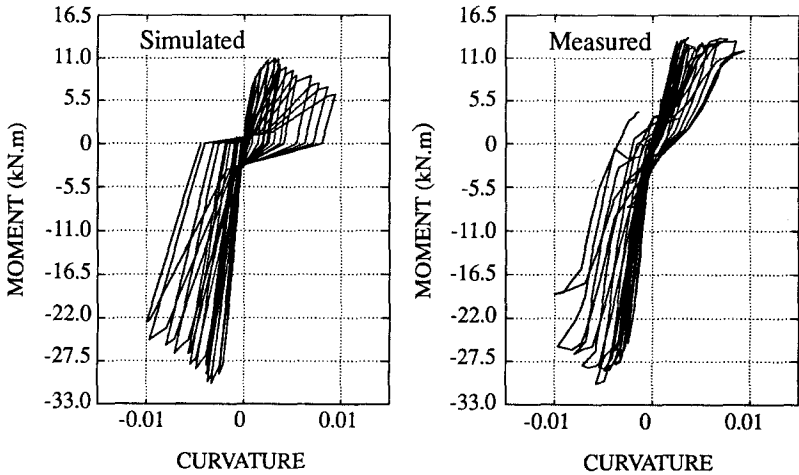
The effective slab-width procedure was originally developed for analyzing two-way slab-column systems for static lateral loads (Pecknold 1975). In this procedure, an effective width factor α_i is obtained such that a slab of width $\alpha_i l_2$ with a uniform rotation at the column support would allow the column located at the center of the panel to rotate the same amount as the original column. The columns are modeled in a conventional manner and the slab is modeled as a beam of effective width $\alpha_i l_2$ with depth equal to the original slab thickness. The effective width factor α_i is calculated based on the equivalent elastic stiffness of the interior slab-column connections. The flexural strength of the slab, which is an important factor in seismic response calculations, is not considered in this approach and the use of the same effective slab-width for both interior and exterior connections is not appropriate.

Equivalent Column Method

In this approach, those portions of the slab attached to the transverse faces of the column are assumed to act as torsional members which transfer moments from the slab to the column. The moment-transfer is assumed to occur directly over the column width c_2 and indirectly along the transverse torsional members. The rotational stiffness of the equivalent column is determined as a function of the torsional stiffness of the transverse members on each side of the joint and the flexural stiffness of the columns above and below the joint. The effect of cracking in the slab is considered indirectly by calibrating the equivalent column stiffness on the basis of experimental data. The full slab width is modeled conventionally and the columns are modeled as equivalent columns. As in the previous case, this procedure is also limited to elastic analysis for gravity and monotonic lateral loads and cannot be used for seismic analysis.



(a) Specimen DNY_3's exterior connection



(b) Specimen DNY_3's interior connection

FIG. 5. Simulated and Measured Moment-Curvature Response of DNY_3: (a) Specimen DNY_3's Exterior Connection; (b) Specimen DNY_3's Interior Connection

PROPOSED EQUIVALENT FRAME APPROACH

Since neither of the previously described approaches is suitable for non-linear analysis of flat plate structures under seismic loading, a modified equivalent frame approach is proposed. This approach is based on the effective slab-width concept which is more convenient for modeling the slab behavior including the strength, stiffness, and hysteretic response.

Effective Slab-Width Factor

The effective slab-width factor α_i is a function of column and slab aspect ratios, and can be calculated by the elastic solution proposed by Pecknold

TABLE 2. Measured and Calculated Moment-Transfer Capacities of Connections

Specimen (1)	EXTERIOR CONNECTION					Interior Connection			
	M_{cf}^a (kN·m) (2)	M_n (kN·m)				M_{cf} (kN·m) (7)	Eq. (1) or Eq. (2) (8)		(column 7)/ (column 8) (9)
		Eq. (1) (3)	(column 2)/ (column 3) (4)	Eq. (3) (5)	(column 2)/ (column 5) (6)				
(a) Negative Bending									
IE	15.8	29.7	0.53	14.5	1.09	—	—	—	—
II	—	—	—	—	—	32.2	34.2	—	0.95
DNY_1	18.9	27.1	0.70	16.0	1.18	31.0	35.1	—	0.88
DNY_2	12.7	26.4	0.48	15.0	0.85	26.3	34.8	—	0.76
DNY_3	18.0	26.3	0.68	14.8	1.21	32.1	34.7	—	0.93
DNY_4	29.0	26.1	1.11	27.5	1.06	30.4	34.2	—	0.89
[Mean]	—	—	0.70	—	1.08	—	—	—	0.88
[Standard deviation]	—	—	0.25	—	0.14	—	—	—	0.07
(b) Positive Bending									
IE	14.6	22.3	0.65	13.1	1.11	—	—	—	—
II	—	—	—	—	—	5.9	11.8	—	0.50 ^b
DNY_1	14.5	16.0	0.90	11.2	1.29	12.3	15.4	—	0.80
DNY_2	7.7	14.9	0.52	9.3	0.84	10.7	13.1	—	0.82
DNY_3	11.9	13.4	0.89	12.7	0.94	14.0	12.9	—	1.09
DNY_4	16.0	12.2	1.31	11.3	1.42	13.4	11.3	—	1.19
[Mean]	—	—	0.86	—	1.12	—	—	—	0.97
[Standard deviation]	—	—	0.30	—	0.24	—	—	—	0.19

^aAverage of moments measured at exterior connections.

^bNot used in mean and standard deviation calculation.

Note: 1 kN·m = 8.85 k-in.

(1975). For the slab-column test specimens considered in the present study, the theoretical values of α_i were calculated as 0.963 for “rigid” columns, and 0.434 for “flexible” columns. The columns in these specimens were designed to remain elastic during the test and thus may be assumed as rigid columns. The elastic effective slab-width factor for the interior connections can thus be taken as 0.963.

Moment-Transfer Capacity of Slab

By assuming the equivalent slab-beam to have the same depth as the original slab and a width of $0.963l_2$, the ultimate strength of the slab in negative bending at both interior and exterior connections can be calculated by

$$M_n = A_{\alpha_i l_2} f_y \left(d - \frac{A_{\alpha_i l_2} f_y}{1.7 \alpha_i l_2 f'_c} \right) \quad (1)$$

and in positive bending by

$$M_n = \frac{1}{6} \alpha_i l_2 h^2 f_r \quad (2)$$

where $A_{\alpha_i l_2}$ = steel top area in the slab-width $\alpha_i l_2$; h = slab depth; and f_r = modulus of rupture of concrete. The calculated and measured flexural strengths of the slab for all specimens are compared in Table 2. Based on the comparison of calculated and measured flexural capacities, the effective slab-width method gives reasonably accurate prediction of the moment-transfer capacity of the slab at interior connections in both positive and negative bending directions. The ratio of measured and predicted moment-

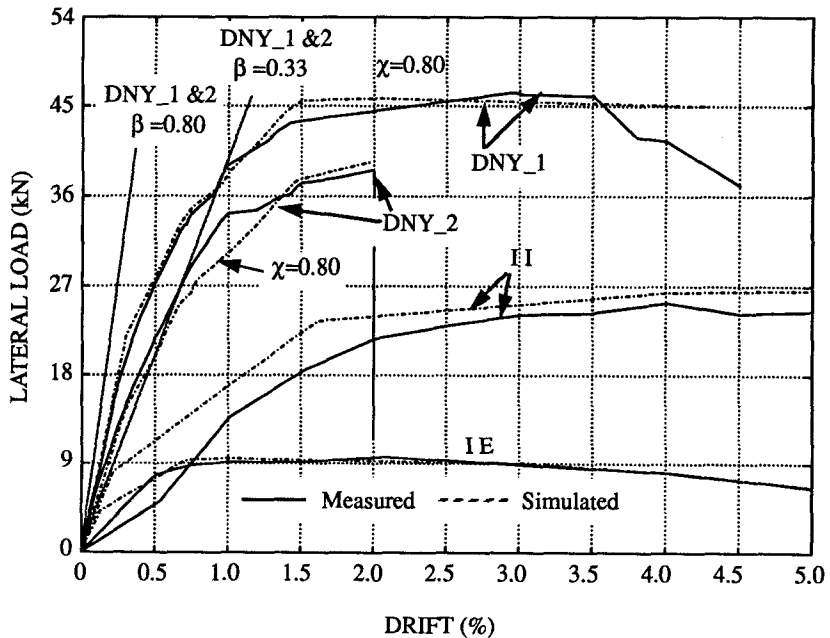


FIG. 6. Comparison of Theoretical and Experimental Results

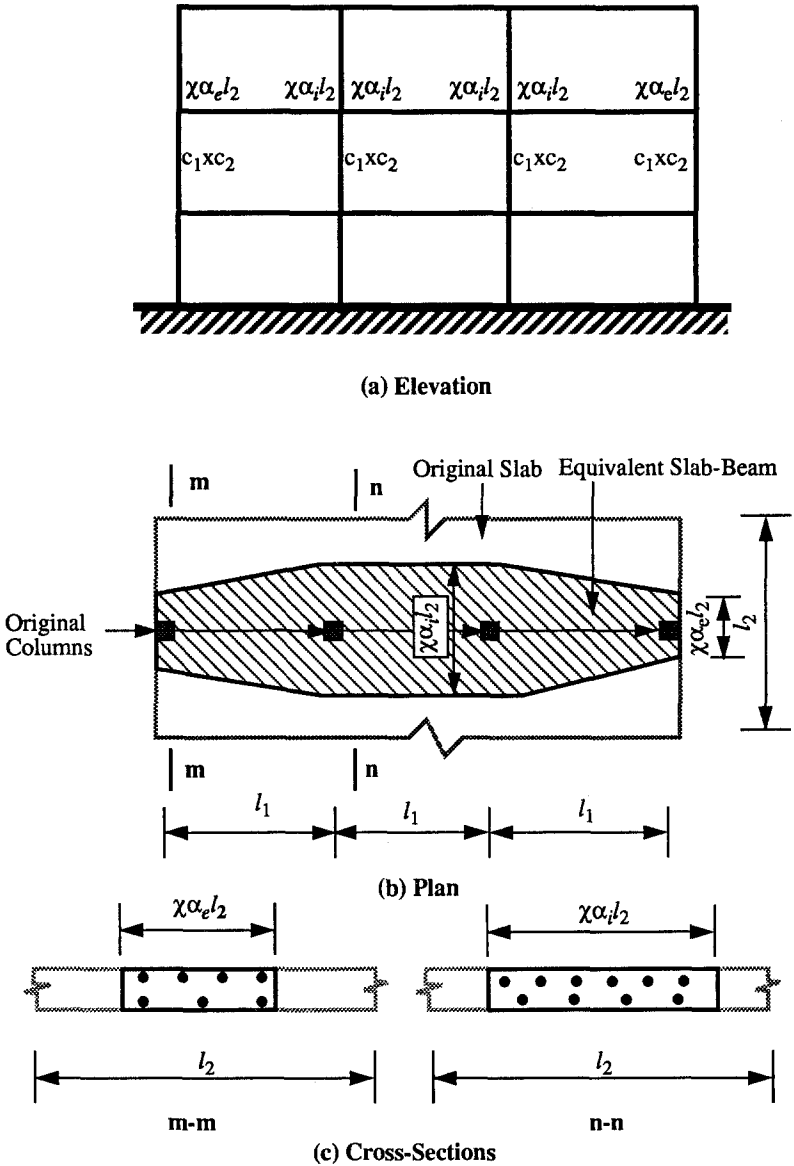


FIG. 7. Equivalent Slab-Width for Flat Plate Frame: (a) Elevation; (b) Plan; (c) Cross Section

transfer capacities in positive bending are between 0.76 and 1.19 except for the specimen II. The measured positive moment-transfer strength of this specimen was low due to cracking of the slab in positive bending prior to the test. For specimen DNY_2, the effective slab-width model overestimates the moment-transfer capacity which suggests that the presence of the heavy gravity load on the slab in DNY_2 reduced the effective slab-width. The theoretical effective slab-width factor α_i , derived for the interior connections

gave a poor prediction of the moment-transfer capacity of the slab at the exterior connections (see column 4 in Table 2). Instead, the moment-transfer capacity of the slab at the exterior connections was predicted more accurately (see column 6 in Table 2) by combining the flexural and torsional strength of the slab as

$$M_n = M_{c_1+c_2} + 2T_c \quad (3)$$

where $M_{c_1+c_2}$ = slab flexural capacity over width $c_1 + c_2$; and T_c = cracking torsional strength of the slab edge.

Effective Stiffness of Interior Connections

Several experimental investigations (Moehle and Diebold 1985; Pan and Moehle 1992; Robertson and Durrani 1992) have shown that the use of gross section properties overestimated the actual stiffness of the slab at interior connections. Vanderbilt and Corley (1983) proposed that the stiffness of the effective slab-width be reduced to one-third of the gross stiffness which gave a lower bound of the lateral stiffness. Based on their experimental results, Pan and Moehle (1992) proposed a similar stiffness reduction factor $\beta = 1/3$. The stiffness reduction factor β accounted for the total loss in stiffness from all causes including cracking and shrinkage. In reality, the stiffness reduction factor is also affected by the gravity load, slab steel ratio, and aspect ratios l_1/l_2 and c_2/l_2 . The behavior of slab-column connections observed during the tests indicated that the stiffness of slab continuously decreased as the lateral drift increased. The assumption of a constant stiffness reduction factor in elastic analysis is thus unrealistic.

For interior connections, the gradual reduction in stiffness of the slab resulting from cyclic lateral loads can be continuously updated as the slab-beam element accumulates more inelastic deformation. The stiffness reduction due to the presence of gravity loads can be accounted for by further reducing the effective width by a factor, χ . The net effective slab-width at interior connections is therefore $\chi\alpha l_2$. Based on the analysis of measured stiffness and moment-transfer capacities of a large number of previously reported slab-column connection tests, the stiffness reduction factor χ for interior connections can be calculated by

$$\chi = 1 - 0.4 \frac{V_g}{4A_c \sqrt{f'_c}} \quad (4)$$

where V_g = total shear at the connection due to gravity load; A_c = area of the slab critical section; and f'_c = compressive strength of concrete in pounds per square inch (psi). The background to this formula and further details can be found elsewhere (Luo and Durrani, in press, 1994). For the slab-column connection subassemblies discussed here, the χ -factor is calculated as 0.80. The stiffness reduction factor χ for the individual specimens is 1.0 as no gravity load was applied to these specimens.

Effective Stiffness of Exterior Connections

As explained earlier, the effective width of slab is different at interior and exterior connections. The model developed by Corley and Jirsa (1970), whereby a part of the total unbalanced moment is transferred in bending from the slab portion connected with front face of the column, and the remainder is indirectly transferred in torsion from the slab connected with

lateral faces of the column, can be used for exterior connections. The torsional stiffness of the slab at the exterior connections is calculated by

$$K_t = \sum \frac{9E_{cs}C}{l_2 \left(1 - \frac{c_2}{l_2}\right)^3} \quad (5)$$

Knowing the slab stiffness in bending and torsion, the equivalent width of the slab at exterior connections can be calculated as

$$\alpha_e l_2 = \frac{K_t}{K_t + K_s} l_2 \quad (6)$$

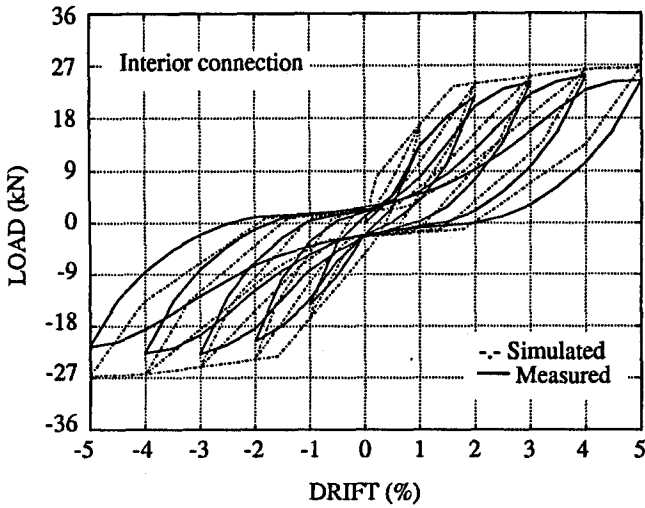
where $K_s = (4E_{cs}I)/l_1 =$ flexural stiffness of the slab framing into the exterior connection. For all subassemblies and individual exterior connections, except DNY_4, which had a spandrel beam, the equivalent width for the slab at the exterior connections was found as $0.78l_2$. For specimen DNY_4, the equivalent slab-width factor α_e was 0.92. The stiffness reduction factor χ for gravity load can be assumed to be the same for both interior and exterior connections.

The load-drift response obtained from linear static analysis for β -values of 0.80 and 0.33, as suggested by other researchers (Vanderbilt and Corley 1983; Pan and Moehle 1992), is shown in Fig. 6. Also shown is the response obtained from the proposed nonlinear equivalent frame analysis approach using an effective slab-width of $\chi\alpha_i l_2$ at interior connections and $\chi\alpha_e l_2$ at exterior connections. The linear elastic approach does not give realistic representation of the actual nonlinear response of the slab-column connections. Furthermore, it may underestimate or overestimate the drift response depending upon the β value chosen. The proposed inelastic equivalent slab-beam model gives a better prediction of the load-drift response over a wide range of drift levels. The initial actual stiffness of specimen II is lower compared with the predicted stiffness due to accidental cracking of the slab prior to the test.

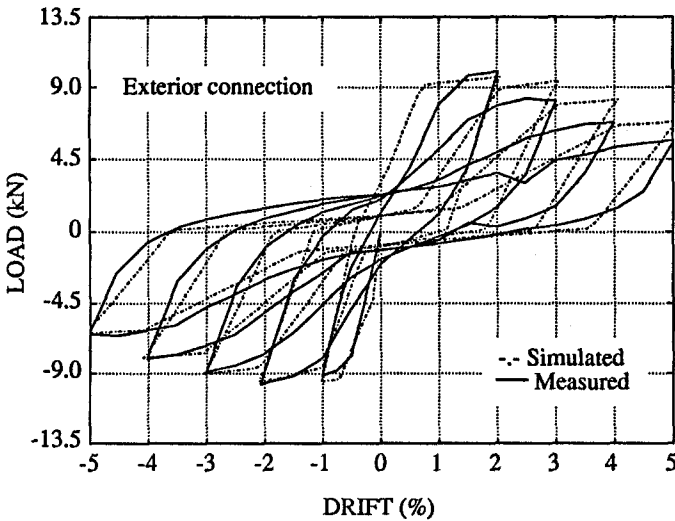
Equivalent Slab-Beam

The proposed definition of the equivalent slab-beam element has different widths at interior and exterior connections, and these widths are determined on the basis of stiffness considerations (Fig. 7). The equivalent slab-widths to match the moment-transfer capacities would be different. In analyzing a frame, it is not possible to define two different widths for the same element to satisfy both strength and stiffness criteria simultaneously. Most of the computer programs, including IDARC-2D, determine element properties from the given dimensions and steel area of the beam element. To overcome this difficulty, the effective width of the slab-beam element is specified as $\chi\alpha_i l_2$ for the interior connections and $\chi\alpha_e l_2$ for the exterior connections to match the observed stiffness and the strength is matched by calculating a new equivalent steel area for the same effective slab-width. For the interior connections, the effective slab-width $\chi\alpha_i l_2$ is found to satisfy both strength and stiffness criteria simultaneously and, therefore, no recalculation of the steel area is required. However, for the slab at the exterior connections, the steel area in the equivalent slab-width needs to be recalculated to achieve the desired moment-transfer capacity

$$M_{\chi\alpha_e l_2} = M_{c_1+c_2} + 2T_c \quad (7)$$



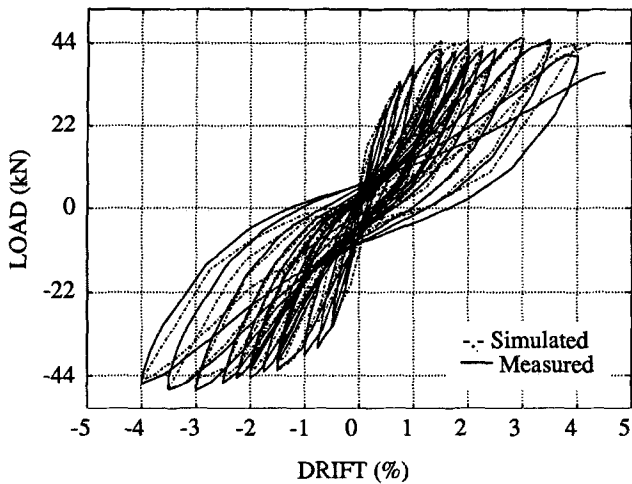
(a) Specimen II



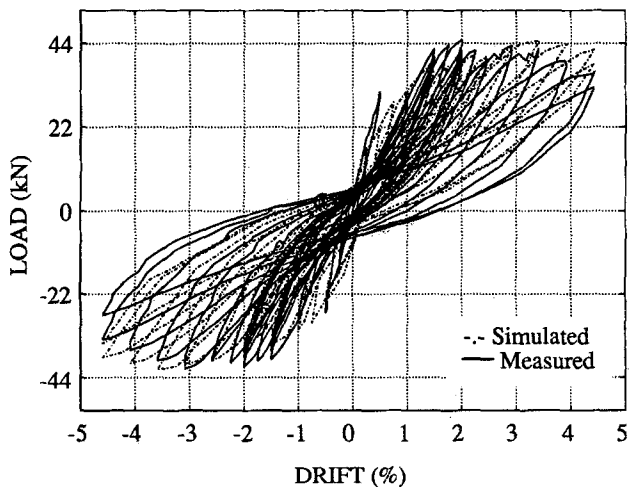
(b) Specimen IE

FIG. 8. Simulated and Measured Load-Drift Response for Individual Connections: (a) Specimen II; (b) Specimen IE

where $M_{\chi\alpha,l_2}$ = nominal strength of the equivalent slab-beam at the exterior connections; T_c = cracking torsional strength of the slab of width c_1 ; and $M_{c_1+c_2}$ = flexural capacity of the slab of width $c_1 + c_2$ centered on the column. The equivalent area of steel can then be calculated by substituting $M_{\chi\alpha,l_2}$ obtained from (7) into the left side of (1).



(a) Specimen DNY_1



(b) Specimen DNY_3

FIG. 9. Simulated and Measured Load-Drift Response for Subassemblies: (a) Specimen DNY_1; (b) Specimen DNY_3

Model Verification

The proposed nonlinear equivalent frame approach is used to simulate the load-drift response of the individual connections and the slab-column connection subassemblies. As shown in Figs. 8 and 9, the proposed approach gives reasonably good agreement between the predicted and the recorded

hysteresis loops. The strength, stiffness, and energy dissipation of the specimens are well matched over the entire cyclic loading routine for both individual connections as well as slab-column connection subassemblies. Based on these results, the proposed approach may be used in evaluating the seismic response of flat plate buildings constructed prior to 1960s with reasonable accuracy.

CONCLUSIONS

Several variations of the equivalent frame method are currently available for analyzing flat plate buildings under combined gravity and static lateral loads. These methods use the effective slab-width approach in which the effective width factor is determined from stiffness compatibility considerations. The effect of cracking in the slab due to gravity and/or seismic load is generally included by assuming a certain stiffness reduction factor which is based mostly on judgment and experience. The building response thus calculated is based on the assumption that the slab stiffness remains constant for the duration of the loading. Laboratory tests of slab-column connection subassemblies have clearly shown that the stiffness continuously degrades as the drift level increases. The elastic response can thus deviate considerably from the actual response depending upon the assumed effective slab-width and the stiffness reduction factor. A nonlinear equivalent frame approach is proposed in which stiffness of the slab is continuously upgraded during calculations. This approach is based on the familiar equivalent slab-beam concept, and it targets both stiffness as well as the moment-transfer capacity of interior and exterior slab-column connections. The effect of cyclic loading is included by using a hysteresis model whose parameters are identified from the measured load-deformation response of slab-column connections. The proposed method is verified by comparing the predicted and measured load-drift response of the slab-column subassemblies. Even though the hysteresis parameters and the effective width factors were identified for flat plate buildings of 1960s vintage, the proposed approach could be equally effectively used for general seismic analysis of flat plate buildings.

ACKNOWLEDGMENTS

The writers wish to acknowledge the support of NCEER (91-3112B and 92-3106C) and the National Science Foundation (Grant No. BCS-9221522) in making this study possible. The views expressed in this paper are those of the writer's and do not necessarily reflect the views of the sponsoring organizations.

APPENDIX I. REFERENCES

- Allen F., and Darvall, P. (1977). "Lateral load equivalent frame." *ACI Struct. J.*, 74(7), 294-299.
- Building code requirements for reinforced concrete; ACI 318-41.* American Concrete Institute (ACI), Detroit, Mich.
- Building code requirements for reinforced concrete; ACI 318-56.* (1956). American Concrete Institute (ACI), Detroit, Mich.
- Building code requirements for reinforced concrete; ACI 318-89.* (1989). American Concrete Institute (ACI), Detroit, Mich.
- Corley, W. G., and Jirsa, J. O. (1970). "Equivalent frame analysis for slab design." *ACI Struct. J.*, 67(11), 875-884.
- Corley, W. G., Sozen, M. A., and Siess, C. P. (1961). "The equivalent frame analysis

- for reinforced concrete slabs." *Struct. Res. Ser. No. 218*, Dept. of Civ. Engrg., University of Illinois, Urbana, Ill.
- Di Stasio, J., and Van Buren, M. P. (1960). "Transfer of bending moment between flat plate floor and column." *ACI Struct. J.*, 57(3), 299–314.
- Durrani, A. J., and Du, Y. (1992). "Seismic resistance of slab-column connections in existing non-ductile flat-plate buildings." *Tech. Rep. NCEER-92-0010*, State University of New York at Buffalo, Buffalo, N. Y.
- Kunnath, S. K., Reinhorn, A. M., and Lobo, R. F. (1992). "IDARC-version 3.0; a program for inelastic damage analysis of reinforced concrete structures." *Tech. Rep. NCEER-92-0022*, State University of New York at Buffalo, Buffalo, N. Y.
- Kunnath, S. K., Reinhorn, A. M., and Park, Y. J. (1990). "Analytical modeling of inelastic seismic response of R/C structures." *J. Struct. Engrg.*, ASCE, 116(4), 996–1017.
- Luo, Y. H. (1993). "Modeling of non-ductile R/C flat-plate buildings," MS thesis, Department of Civil Engineering, Rice University, Houston, Tex.
- Moehle, J. P., and Diebold, J. W. (1985). "Lateral load response of flat-plate frame." *J. Struct. Engrg.*, ASCE, 111(10), 2149–2163.
- Pan, A. D., and Moehle, J. P. (1992). "An experimental study of slab-column connections." *ACI Struct. J.*, 89(6), 626–638.
- Park, R., and Islam, S. (1976). "Strength of slab-column connections with shear and unbalanced flexure." *J. Struct. Engrg.*, ASCE, 102(9), 1879–1901.
- Pecknold, D. A. (1975). "Slab effective width for equivalent frame analysis." *ACI Struct. J.*, 72(4), 135–137.
- Robertson, I. N., and Durrani, A. J. (1992). "Gravity load effect on seismic behavior of connections in indeterminate interior slab-column connections." *ACI Struct. J.*, 89(1), 37–44.
- Uniform Building Code*. (1991). International Conference of Building Officials, Whittier, Calif.
- Vanderbilt, M. D., and Corley, W. G. (1983). "Frame analysis for concrete buildings." *Concrete Int.: Design & Constr.*, 5(12), 33–43.

APPENDIX II. NOTATION

The following symbols are used in this paper:

- A_c = area of slab critical section as defined in ACI 318–89;
- $A_{\chi\alpha,l_2}$ = steel area in equivalent slab-beam of width $\chi\alpha l_2$;
- A_{α,l_2} = steel area in equivalent slab-beam of width αl_2 ;
- C = cross-sectional constant for torsional section property;
- c_1 = column dimension in bending direction;
- c_2 = column dimension normal to bending direction;
- d = effective depth of slab;
- E_{cs} = modulus of elasticity of slab concrete;
- f_c^t = compressive strength of concrete;
- f_r = modulus of rupture of concrete;
- f_y = yielding strength of steel;
- h = slab thickness;
- I = moment of inertia of slab;
- K_s = flexural stiffness of slab;
- K_t = torsional stiffness;
- l_1 = span length in bending direction, center-to-center of columns;
- l_2 = span length in direction transverse to l_1 , center-to-center of columns;
- M_{cf} = measured flexural strength of slab at column face;
- $M_{c_1+c_2}$ = flexural capacity of slab of width $c_1 + c_2$ centered on column;

- M_n = nominal flexural strength of slab;
 $M_{\chi\alpha_e l_2}$ = nominal flexural strength of equivalent slab-beam at exterior connection;
 T_c = cracking torsional strength of slab edge of width c_1 ;
 V_g = total shear at connection due to gravity load;
 α = stiffness degrading coefficient;
 α_e = effective slab-width factor for slab at exterior connection;
 α_i = effective slab-width factor for slab at interior connection;
 β = linear stiffness reduction factor;
 β_1 = energy-based deteriorating coefficient;
 β_2 = ductility-based deteriorating coefficient;
 γ = target slip or crack-closing parameter; and
 χ = stiffness reduction factor for gravity load.